2

Theoretical aspects: a mathematical background

This chapter addresses basic mechanisms and mathematical models related to droplet wetting phenomena and dynamics. It includes discussions on the effects of surface roughness employing the modified Wenzel and Cassie equations. The phenomena of electrowetting on dielectric (EWOD) and contact angle saturation (CAS) aspects are also highlighted.

2.1 Introduction

In this chapter, we delve into the theoretical frameworks from hydrophilicity to superhydrophobicity. Initially, we explore the Young's model for smooth surface and further, modified model for textured surfaces, i.e., Wenzel and Cassie models [100]. To elucidate the dynamics of droplet on slanted textured surfaces under gravitational force, the concept of contact angle hysteresis (CAH) is discussed [101]. The interplay of surface tension in both static and dynamic droplet behavior has spurred interest in controlling droplet motion. Numerous methods exist to manipulate droplet movement on solid surfaces, including the application of external forces such as pressure [102], temperature [103], magnetic fields [104], and electric fields [105, 106]. Among these methods, electric field-induced droplet manipulation stands out due to its numerous advantages. We will address mathematical models, focusing specifically on electric field-induced wetting, also known as the electrowetting phenomenon. The wettability of liquids on surfaces depends on numerous factors corresponding to wetting states. Wetting states are determined by the interfacial surface tension between two phases, whether they are of different phases (e.g., liquid-solid) or of same phases (liquid-liquid). Understanding how liquids can wet a solid surface or not is enhanced by examining the balance of surface tension forces per unit length at the three-phase contact line between solid, liquid, and gas phases .

2.2 Spreading and wettability of liquids

2.2.1 Liquid spreading

The spreading of liquid (water) on solid/immiscible liquid surface depends on interfacial tension between three pairs of phases: solid, liquid, and air ($\gamma_{\mathrm{SL}}, \gamma_{\mathrm{LA}}, \gamma_{\mathrm{SA}}$). In general, the interfacial tension between two phases can be presented by γ_{ij}, is the free energy required to increase per unit contact area of two phases i and j. Suppose a liquid droplet is placed on a solid surface, the state of wetting of solid can be determined by spreading parameter, S, which is the difference between surface energy per unit area of non-wetted to wetted solid surface. Mathematically, it can be stated as [107, 108];

$$S = \gamma_{\mathrm{SA}} - (\gamma_{\mathrm{SL}} + \gamma_{\mathrm{LA}}). \tag{2.1}$$

Clearly, Eq. (2.1) falls in two cases:

• For S $>$ 0, i.e., the liquid will tend to spread out over the solid surface and results total wetting.

• For S $<$ 0, i.e., the liquid will try to spread on solid surface but at equilibrium, it will remain as a spherical drop, and results partial wetting.

2.2.2 Contact angle (CA) and Young's equation (1805)

Wetting equation relates the contact angle (CA) of liquid on solid in air (or a solid and two immiscible liquid) medium. The Fig. 2.1 depicts the partial wetting liquid on smooth solid surface. Let us consider the three phases (solid, liquid, and air) are in contact with surface tensions $\gamma_{\mathrm{SL}}, \gamma_{\mathrm{LA}}$, and γ_{SA}, respectively. The surface tension force act at three phase contact line (TCL) where solid, liquid and air (or immiscible liquid 2) meets Figs 2.1(a) and 2.1(b). The angle formed between solid -liquid and liquid -air tangents, known as Young's contact angle. The value of CA can be determined by mechanical equilibrium of forces per unit length at TCL. At equilibrium, the horizontal force balance at TCL is given by [109];

$$\gamma_{SA} = \gamma_{SL} + \gamma_{LA} \cos\theta_Y, \tag{2.2}$$

$$\text{or,} \quad \cos\theta_{\mathrm{Y}} = \frac{\gamma_{\mathrm{SA}} - \gamma_{\mathrm{SL}}}{\gamma_{\mathrm{LA}}}. \tag{2.3}$$

The Eq. (2.3) known as *Young–Dupré* equation, or *Young's* equation. Where θ_Y is the CA of liquid on solid surface at TCL. Using Eqs. (2.1) and (2.2), re-written

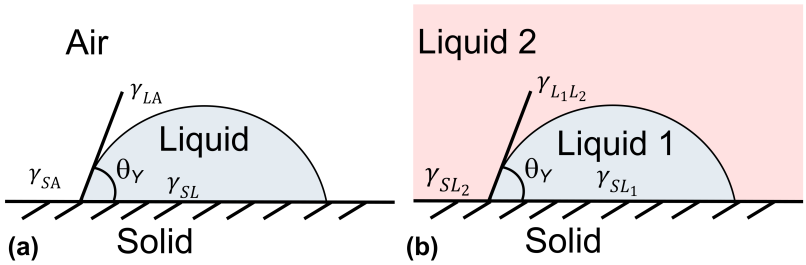

Figure 2.1: Schematic illustration of wetting of liquid on solid.(a) Air medium. (b) Immiscible liquid medium.

Eq. (2.3) as [110, 111],

$$\cos\theta_Y = 1 + \frac{S}{\gamma_{\mathrm{LA}}}. \tag{2.4}$$

The Eq. (2.4) is simply Young's equation in terms of spreading parameter. Upon making inspection of Eq. (2.4), we can observe that, if $S \geq 0, \cos\theta_Y \geq 1$. It implies that θ_Y will be undefined and total spreading results. Again, if $S < 0$ then θ_Y undergoes partial wetting state [112]. It should be noted here, the Eq. (2.2) is derived under partial wetting assumption and therefore, Young's CA must lie in between 0^o and 180° values, i.e., $\cos\theta_{\mathrm{Y}} \in (-1, 1)$.

In other words, If $\gamma_{\mathrm{SG}} > \gamma_{\mathrm{SL}}$ then $\theta_Y < \frac{\pi}{2}$, the liquid will form acute angle which can be termed as liquiphilic surface. That is, the surface tension force at interface between solid and liquid laser than liquid -air interface. If $\gamma_{\mathrm{SA}} < \gamma_{\mathrm{SL}}$ then $\theta_Y < \frac{\pi}{2}$, the liquid will form acute angle which can be termed as liquiphilic surface. If $\gamma_{\mathrm{SG}} < \gamma_{\mathrm{SL}}$, then $\theta_Y > \frac{\pi}{2}$, that is the liquid will form an obtuse CA and then a such surface will be known as liqiphobic. It should be noted that in case of water liquid, such surfaces are known as, hydrophilic and hydrophobic; respectively. However, for oil liquids, known as oleophilic and oleophobic surfaces of respective terms.

Important points:

• For a rigid solid surface, the vertical force component is unbalanced, however, negligible effect can be considered for soft elastic solid/liquid surfaces which deform under vertical force component ($\gamma_{\mathrm{LA}} \sin\theta$).

• For any stable CA, Eq. (2.3) must hold the inequality, $|\gamma_{\mathrm{SA}} - \gamma_{\mathrm{SL}}| \leq \gamma_{\mathrm{LA}}$.

• The γ_{ij} must be positive, otherwise the interface of two phases would increase and will mix, i.e., no longer interface will exist.

• The Eq. (2.3) can also be derived through energy minimization. If a liquid drop is in an equilibrium state, it is in the minimum surface energy configuration. Suppose δE is the variation of the surface energy by moving dx amount of TCL along solid -air interface. From Fig. 2.2(a), the resulting variation of the three-phase interfacial energy will be given by [32];

$$\delta E = dx(\gamma_{\mathrm{SL}} - \gamma_{\mathrm{SA}} + \gamma_{\mathrm{LA}} \cos\theta_Y). \tag{2.5}$$

At equilibrium, $(\frac{d\delta E}{dx} = 0)$, which implies, $\cos\theta_Y = \frac{\gamma_{\mathrm{SA}} - \gamma_{\mathrm{SL}}}{\gamma_{\mathrm{LA}}}$. This is the desired Young's equation.

• In a system where all three phases possess elasticity and there are no solid surfaces present, such as an oil droplet on a water film in an air medium, the interfaces experience deformation. At the juncture where the three phases intersect, the equilibrium of the three tangential surface tension forces results in the formation of a triangular like shape known as the Neumann triangle, which establishes a relationship of characteristic CA's formed between interfacial surface tension forces of three phases body. In such case, to determine CA's, taking the vector sum of all three-surface tension forces at TCL as shown in Fig. 2.2(b) , is given by [113, 114];

$$\sum_{\substack{i,j=1 \\ i \neq j}}^{3} \gamma_{ij} = 0. \tag{2.6}$$

Using trigonometric sine rule,

$$\frac{\gamma_{12}}{\sin\theta_1} = \frac{\gamma_{23}}{\sin\theta_2} = \frac{\gamma_{13}}{\sin\theta_3}. \tag{2.7}$$

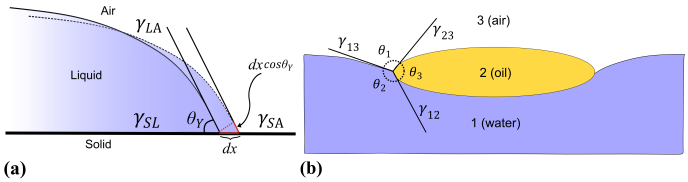

Figure 2.2: Schematic represents the wetting state of a liquid (a) on solid surface and (b) on an immiscible liquid surface.

2.3 Wettability of single level surface texture

2.3.1 The Wenzel model (1936)

Young's law, originally applicable only to smooth surfaces, falls short in describing the behavior of liquids on textured solid surfaces, which are abundant in nature. In 1936, Wenzel proposed a straightforward model to examine the wetting characteristics of such textured surfaces, revealing differences in CA's compared to smooth surfaces. Consequently, roughening solid surfaces emerges as a viable method to modulate their hydrophobic or hydrophilic properties. Suppose a perfectly smooth solid surface with

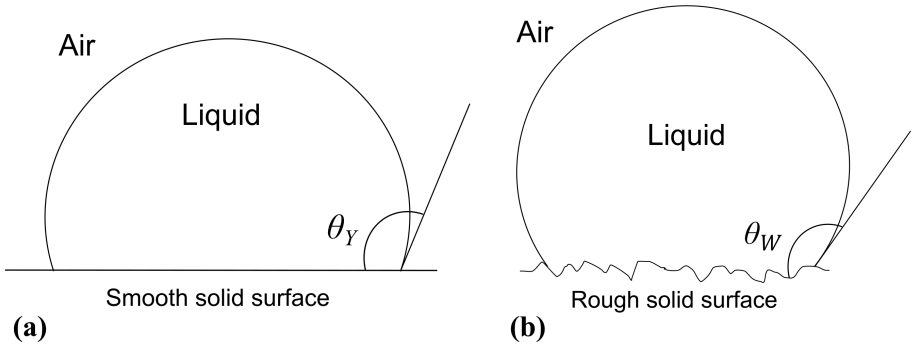

Figure 2.3: Schematic illustration of wetting state of liquid on solid. (a) On smooth surface. (b) Rough surface.

CA $= \theta_Y$, then the change in CA due to surface roughness is given by [115, 116];

$$\cos\theta_W = r_\phi \cos\theta_Y, \tag{2.8}$$

here, r_ϕ is the dimensionless roughness factor introduced by Wenzel, defined as the ratio of the actual wetted area to the projected area, which is always greater than 1 [117].

From Eq. (2.8), The dependence of the CA on the surface roughness compared to smooth one is depicted in Figs. 2.3(a) and 2.3(b). The Wenzel model estimate the enhanced CA due to surface texture. In general, for a hydrophobic solid surface, roughness induces more hydrophobicity, while a hydrophilic solid surface becomes more hydrophilic, i.e., for surfaces, if $\theta_Y > 90^\circ$ then, $\theta_W > \theta_Y$; $\theta_Y < 90^\circ$ implies $\theta_W < \theta_Y$. In the Wenzel wetting state, the pores are completely filled with liquid, leaving no air pockets at the solid-liquid interface. This state is often referred to as the collapsed wetting state.

2.3.2 The Cassie -Baxter model (1944)

The Wenze model describes the equilibrium CA on a rough solid surface, but the Wenzel equation becomes insufficient when addressing solid surfaces with intricate characteristics, like porosity or diverse chemical compositions. It is limited in explaining liquid-filled rough surfaces [118]. However, numerous textured surfaces in nature show extraordinary water contact angles (WCA). Such surfaces possess air-filled pores that resist water filling the texture, resulting in minimal liquid-solid contact area.

In 1944, Cassie proposed a model by considering surface chemical heterogeneity and introducing a parameter called, solid-liquid fraction and thereby offering a more inclusive framework. Suppose a surface is composed of two different chemically solids, say solid 1 and solid 2. The fractional area of solids is f_1 and f_2 such that $f_1 + f_2 = 1$ with CA's θ_1 and θ_2 respectively, as shown in Fig. 2.4(a). The apparent contact angle

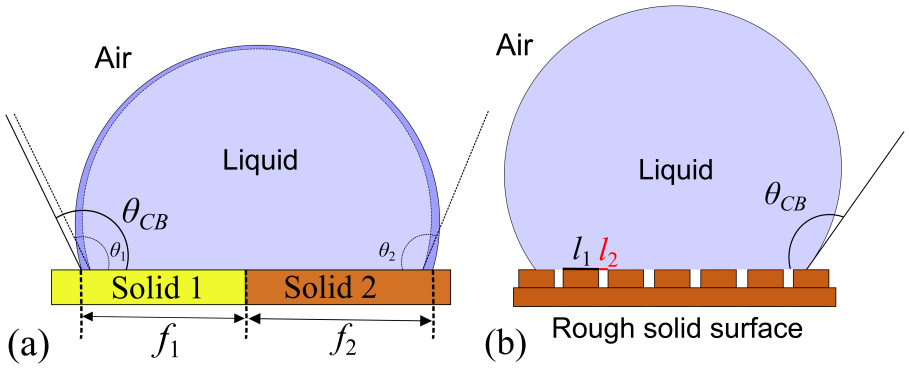

Figure 2.4: Schematic illustration of wetting state of liquid on solids. (a) Two chemically different solids. (b) Rough surface with air pockets.

(θ_{CB}) is given by the Cassie-Baxter equation [119–121];

$$\cos\theta_{\mathrm{CB}} = f_1 \cos\theta_1 + f_2 \cos\theta_2. \tag{2.9}$$

In general, we can write solid surfaces with n chemical compositions [122],

$$\cos\theta_{\mathrm{CB}} = \sum_{i=1}^{n} f_i \cos\theta_i, \tag{2.10}$$

where θ_i is the CA associated with the solid surface of ith chemical composition. The solid-liquid fraction $f_1 + f_2 + f_3 + \ldots + f_n = 1$. If the solid surface is composed of a single material but contains air pockets, as shown in Fig. 2.4(b), suppose f_1 for the solid surface and f_2 for the air pocket fractions, respectively. The CA on the solid surface is $\theta_1 = \theta_Y$ and for air $\theta_2 = 180°$. Using Eq. (2.9),

$$\cos\theta_{\mathrm{CB}} = f_1 \cos\theta_Y - f_2, \tag{2.11}$$

$$\text{or} \quad \cos\theta_{\mathrm{CB}} = f_1(1 + \cos\theta_Y) - 1. \tag{2.12}$$

Where, θ_Y is the Young's contact angle on a smooth solid surface. The solid-liquid and liquid-air fractions are $f_1 = \frac{l_1}{l_1+l_2}$ and $f_2 = \frac{l_2}{l_1+l_2}$, respectively. If the liquid-trapped air length l_2 becomes zero, i.e., $f_1 = 1, f_2 = 0$, from Eqs. (2.11) and (2.12), the apparent contact angle θ_{CB} will become Young's contact angle, θ_Y.

2.4 Wettability of dual (micro-nano) surface texture

2.4.1 Composite/mixed wetting states

Natural and artificial surfaces featuring dual roughnesses maintain high CAs for extended periods compared to those possessing single level of roughness. The phenomenon of mixed state is particularly evident when the solid surface exhibits micro-nano structures across two distinct roughness scales. By employing the Wenzel and Cassie models, one can assess the interface configurations associated with various possible wetting states. Consider a scenario where the microstructure is adorned with nano-scale roughness [123, 124]. By analysing the sustainability of Laplace pressure across the confined pore air-liquid (water) interface, one can discern four potential wetting states contingent upon the optimized density of surface texture. The theoretical basic combination of Wenzel and Cassie wetting states, Wenzel-Wenzel state, Cassie-Wenzel state, Wenzel-Cassie state, and Cassie-Cassie state were depicted schematically in Fig. 2.5. The relationship for Wenzel and Cassie wetting states are described through Figs. 2.5(a) and 2.5(b), Eqs. (2.8) and (2.12). Suppose f_M, f_N, and r_M, r_N are micro, nano solid-liquid fraction and ratio of actual to projected area, respectively. When a liquid droplet is placed on micro texture covered with nano texture then distinctly different composite states emerge. Let us consider a scenario where micro and nano pores are filled by liquid droplet, i.e., Wenzel-Wenzel wetting state, shown in Fig. 2.5(c). In this case, the variation of the surface free energy due to displacement dx amount of TCL, is given by he change in energy dE [27]:

$$dE = \gamma_{\mathrm{LA}} \cos\theta_{\mathrm{WW}}\, dx + (r_M + r_N - 1)(\gamma_{\mathrm{SL}} - \gamma_{\mathrm{SA}})\, dx. \tag{2.13}$$

At equilibrium, $\frac{dE}{dx} = 0$, and using Eq. (2.3), the apparent contact angle θ_{WW} is given by:

$$\cos\theta_{\mathrm{WW}} = (r_M + r_N - 1)\cos\theta_Y. \tag{2.14}$$

Similarly, using surface free energy minimization of the system, we get the following relationships [27], as shown in Figs. 2.5(d-f).

• Cassie-Wenzel state:

$$\cos\theta_{\mathrm{CW}} = f_M(r_N \cos\theta_Y + 1) - 1. \tag{2.15}$$

To illustrate composite wettability, let us assume that f_M, f_N, are micro, nano solid-liquid fractions, $0 < f < 1$ and r_M, r_N are Wenzel roughness (r_ϕ>1) for micro, nano textures, respectively.

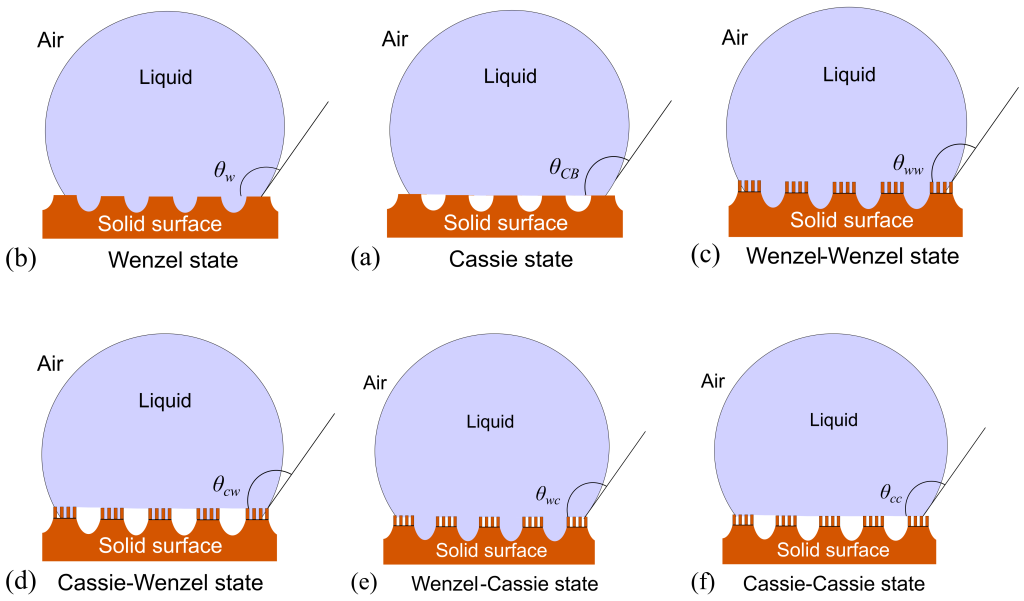

Figure 2.5: Illustrations of liquid droplet configurations in collapsed or suspended wetting states on micro/nano posts are shown. (a) Cassie state. (b) Wenzel state. (c) Wenzel-Wenzel state. (d) Cassie-Wenzel state. (e) Wenzel-Cassie state. (f) Cassie-Cassie state.

- Wenzel-Cassie state:

$$\cos\theta_{\mathrm{WC}} = (f_N + r_M - 1)\cos\theta_Y + f_N - 1, \tag{2.16}$$

$$\text{or} \quad \cos\theta_{\mathrm{WC}} = \cos\theta_c^N + (r_M - 1)\cos\theta_Y, \tag{2.17}$$

here, θ_c^N is the Cassie contact angle of nano-texture part.

- Cassie-Cassie state:

$$\cos\theta_{\mathrm{CC}} = f_N f_M(\cos\theta_Y + 1) - 1. \tag{2.18}$$

2.4.2 Dynamic CA measurements and contact angle hysteresis (CAH)

As previously noted, the Young's relation does not incorporate the volume dependence of CA at equilibrium for liquid droplets. It has been observed that when a droplet attains equilibrium on a solid surface and its size subsequently decreases or increases, this leads to specific changes in dynamic CA, results the advancing or receding CAs as shown in Fig. 2.6(a). From these correlations, we deduce that advancing CA serves as a metric for surface dewetting (repellency) while receding CA indicates surface wetting (adhesion) features [23]. The CAH is defined as the

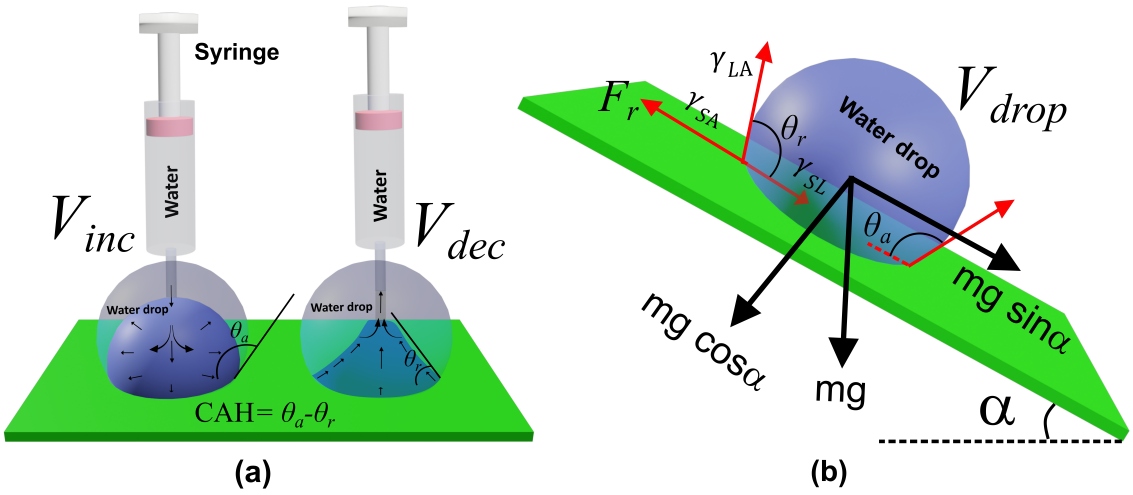

Figure 2.6: (a) Schematics for advancing (θ_a) and receding (θ_r) contact angles corresponding to the increasing and decreasing droplet size. (b) Droplet equilibrium dynamics with tilt angle (α) of the substrate. Here mg being droplet's weight and V_{drop} is the droplet volume.

difference between advancing (θ_a) and receding (θ_r) contact angles, and is given by [23];

$$\Delta\theta_{\text{CAH}} = \theta_a - \theta_r. \tag{2.19}$$

In equilibrium, the CA of a liquid droplet on a solid surface (θ_Y) can vary between (θ_a) and (θ_r). Hysteresis is often linked to surface chemical or structural heterogeneities of solid surface, although there exists some debate regarding the precise connection and consensus that hysteresis arises from pinning at the TCL. Further, if the liquid droplet-substrate system is slanted from $0° - 90°$, the droplet will pin the surface before reaching the roll-off angle. The difference between maximum θ_a and corresponding minimum θ_r will give CAH, as shown in Fig. 2.6(b).

2.5 Droplet rolling and bouncing mechanism

2.5.1 Sessile droplet on inclined plane

As illustrated in Fig. 2.6(b), Furmidge's equation can be used to describe the relationship between the rolling droplet and the tilting angle, excluding the effect of droplet depinning [125]. However, *Brown et al.* explained the depinning of a static water droplet with respect to the tilting angle. The tangential force due to gravity along the inclined surface, known as the pinning force on the droplet, can be expressed as follows [126]:

$$F_p = mg \sin\alpha. \tag{2.20}$$

In this context, mg represents the weight of the liquid droplet, while α denotes the surface tilting angle. When the droplet is in equilibrium on an inclined surface, the force acting on it is balanced by the surface tension along the TCL [127]. This line marks the intersection of the liquid-air interface with the solid surface, thus resulting in a pinning force, which can be expressed as:

$$F_p = D_{TCL}\gamma_{LA}(\cos\theta_r - \cos\theta_a). \tag{2.21}$$

The angles θ_r and θ_a characterize receding and advancing WCAs with tilting angle, α. On combining Eqs. (2.20) and (2.21), one would obtain a requisite criterion for the droplet roll-off with tilting angle . It should be noted here, the D_{TCL} is contact line length normal to the direction of droplet motion of TCL. Therefore [128];

$$\sin\alpha = \frac{2D_{TCL}\gamma_{LA}(\cos\theta_r - \cos\theta_a)}{\pi mg}. \tag{2.22}$$

Here, the coefficient $\frac{2}{\pi}$ originates from the shape of the droplet. As the inclination angle increases, it may eventually reach a critical point where the surface tension force can no longer support the droplet's weight. At the TCL, static equilibrium is lost, prompting the droplet to roll down the inclined surface. This specific angle where it starts rolling is referred as the roll-off angle.

2.5.2 Droplet impact on solid surface

The dynamics of droplet impact rely on numerous variables. Therefore, before delving into bouncing behavior, it's essential to establish the fundamental definitions of some basic parameters. Suppose a liquid droplet characterized by characteristic length l, density ρ, dynamic viscosity $\mu = \rho\nu$, and surface tension γ, falls under gravitational acceleration g with velocity u. This scenario involves six physical variables: l, ρ, ν, γ, g, and u, which can be described using three fundamental units: mass, length, and time. According to Buckingham's Theorem, any system with M physical variables (here, l, ρ, ν, γ, g, and u) expressed in N fundamental units (mass, length, time) will have $M - N$ dimensionless groups that describe the system. In this case, 6 - 3 = 3. Therefore, the theorem suggests that the system can be uniquely characterized by three different dimensionless parameters, defined as follows [129]:

$$\text{Reynolds number } (Re) = \frac{ul}{\nu} = \frac{\text{Inertia}}{\text{Viscosity}}. \tag{2.23}$$

$$\text{Froude number } (Fr) = \frac{u^2}{gl} = \frac{\text{Inertia}}{\text{Gravity}}. \tag{2.24}$$

$$\text{Bond number } (Bo) = \frac{\rho g l^2}{\gamma} = \frac{\text{Gravity}}{\text{Curvature}}. \tag{2.25}$$

Using Eqs. (2.23), (2.24), and (2.25), one can derive important dimensionless parameters as follows [129]:

$$\text{Weber number } (We) = \frac{\rho u^2 l}{\gamma}. \tag{2.26}$$

$$\text{Capillary number } (Ca) = \frac{\rho \nu u}{\gamma}. \tag{2.27}$$

Moreover, the energy dissipation factor holds significance in understanding the rebound characteristics of a liquid droplet. This factor is quantified by the restitution coefficient, denoted as $e = \frac{u_r}{u_i}$, where u_r and u_i represent the velocities of the reflected and impacting droplets on the solid surface, respectively [130]. Upon impact with a solid surface as illustrated in schematic Fig. 2.7, a droplet initially undergoes spreading, assuming a pancake-like shape. Subsequently, it may retract or remain in place, contingent upon the nature of the solid surface. The droplet's potential energy is converted into kinetic energy, with significant energy dissipation attributed to liquid viscosity [131]. The Reynolds number (Eq. (2.23)) delineates the dissipation of energy due to viscosity and its storage in surface tension. Additionally, the CAH (Eq. (2.19)) represents another parameter linked to chemical and structural heterogeneity, serving as a source of energy dissipation. Essentially, whether the droplet fully or partially rebounds depends on its physical properties, the surface construct of the solid base, impact velocity, and other contributing factors.

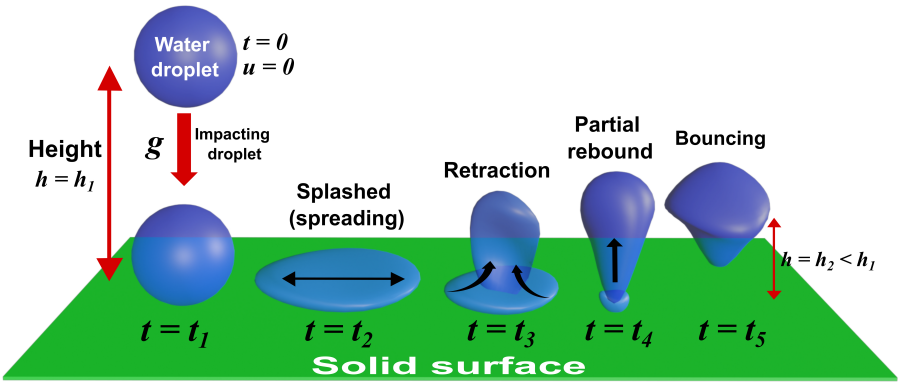

Figure 2.7: Schematics illustrate the impact of a droplet on a solid surface.

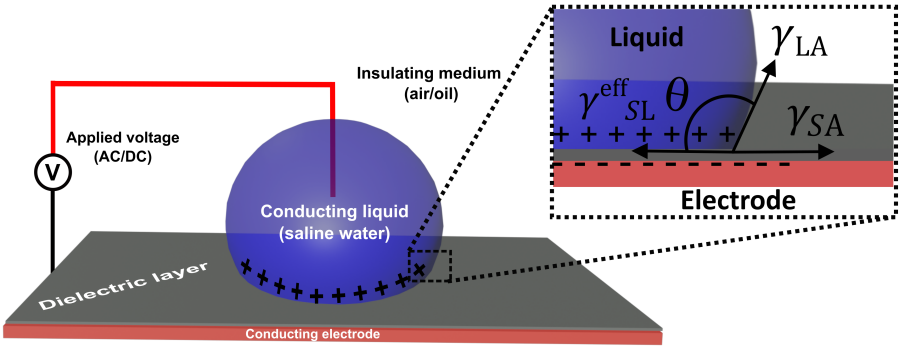

Figure 2.8: The schematics illustrate the EWOD configuration used to manipulate droplets with electric fields.

2.6 Electrowetting and magnetowetting

2.6.1 Electrowetting on dielectric (EWOD)

Suppose a conducting (ionic) liquid drop is at equilibrium on conductive electrode coated with a thin dielectric layer. Now if a voltage, V_{app} is applied across electrodes (Fig. 2.8), the change in the effective solid-liquid interfacial surface tension is given by [132–135];

$$\gamma^{\text{eff}}_{\text{SL}}(V_{\text{app}}) = \gamma_{\text{SL}} - \int_0^{V_{\text{app}}} \sigma_{\text{SL}}\, dV, \tag{2.28}$$

$$\text{or,} \quad \gamma^{\text{eff}}_{\text{SL}}(V_{\text{app}}) = \gamma_{\text{SL}} - \int_0^{V_{\text{app}}} CV\, dV, \tag{2.29}$$

$$\text{or,} \quad \gamma^{\text{eff}}_{\text{SL}}(V_{\text{app}}) = \gamma_{\text{SL}} - \frac{1}{2}CV^2_{\text{app}}. \tag{2.30}$$

Where, σ_{SL} is the surface charge density at interface, $C = \frac{\varepsilon_0\varepsilon_r}{2d}$ is the capacitance, ε_0 is the permittivity of vacuum $\sim 8.854\times10^{-12}$ F/m, and ε_r is the relative permittivity of the dielectric layer of thickness d. Using Eq. (2.30), the Young's Eq. (2.3) can be given by [32, 74],

$$\cos\theta(V_{\text{app}}) = \frac{\gamma_{\text{SA}} - \gamma^{\text{eff}}_{\text{SL}}(V_{\text{app}})}{\gamma_{\text{LA}}}, \tag{2.31}$$

$$\text{or,} \quad \cos\theta(V_{\text{app}}) = \cos\theta_Y + \frac{\varepsilon_0\varepsilon_r}{2\gamma_{\text{LA}}d}V^2_{\text{app},} \tag{2.32}$$

$$\text{or,} \quad \cos\theta(V_{\text{app}}) = \cos\theta_Y + \eta. \tag{2.33}$$

Here, $\theta(V_{\text{app}})$ is the CA after applied voltage V_{app}, and that $\eta = \frac{\varepsilon_0\varepsilon_r}{2\gamma_{\text{LA}}d}V^2_{\text{app}}$ is the electrowetting number. It should be noted that we have assumed that is no potential at zero charge. The Eq. (2.33) known as Lippmann-Young's law.

2.6.1.1 Contact angle saturation (CAS)

According to Eq. (2.33), the CA must vanish at certain applied voltage, i.e., $\theta = 0$, at $V_{\text{app}} = V_{\text{cri}}$ (critical applied voltage). It has been observed that the Lippmann-Young's equation is limited to explain CA with high applied voltage region [136]. If the applied voltage increases, the decrease in CA will stop at certain applied voltage, i.e., $\theta = \theta_s at$ at $V_{\text{app}} = V_{\text{sat}}$, here θ_{sat} is the saturation CA at applied saturation voltage (V_{sat}), Fig. 2.9. Currently, various theories have been suggested to account for the saturation limit. However, there are limited known facts regarding the real phenomena underlying the CA saturation, and the debate is still open [137]. Various models have been proposed to elucidate the phenomenon CAS, including hypotheses involving, the zero solid surface-liquid interface energy [138], charge trapping within dielectrics [134, 139], electrical resistance within the conducting liquid [140], the fringe effect of electric fields [141], and other experimental frameworks [142]. Here, we will discuss the zero solid surface-liquid energy limit to explain the CAS. For a zero voltage, the force balance is that defined by the classical Young's law, Eq. (2.3). As the applied voltage increases, the effective solid-liquid surface tension ($\gamma_{\text{SL}}^{\text{eff}}$) decreases, and the CA decreases according to Eq. (2.33). As we have mentioned earlier, the lower limit for the surface tension is zero. Suppose at the applied voltage, Vapp = Vsat, the effective solid-liquid surface tension become zero, i.e., using Eq. (2.30) [138], $\gamma_{\text{SL}}^{\text{eff}}(V_{\text{app}})\Big|_{V_{\text{app}}=V_{\text{sat}}} = 0$. According to Eq. (2.31), at saturation [113],

$$\cos\theta_{\text{sat}}\Big|_{V_{\text{app}}=V_{\text{sat}}} = \frac{\gamma_{\text{SA}}}{\gamma_{\text{LA}}}. \tag{2.34}$$

$$\theta_{\text{sat}} = \arccos\left(\frac{\gamma_{\text{SA}}}{\gamma_{\text{LA}}}\right). \tag{2.35}$$

The Eq. (2.35) require the information of the solid surface tension, however it is rather difficult to determine, to predict the CAS.

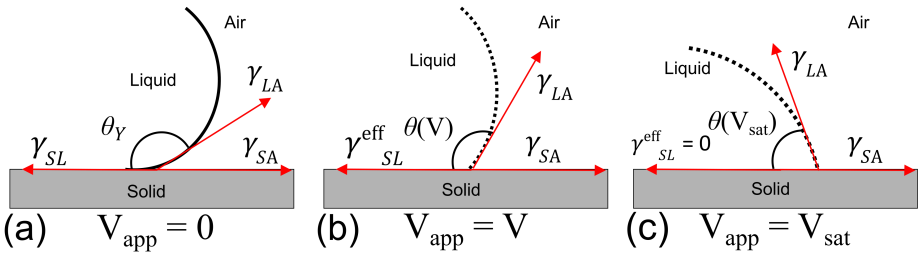

Figure 2.9: The schematic illustrates CAS for applied voltages in the EWOD system, showing how high voltage affect droplet CA behavior.

2.6.2 Magnetowetting

When a magnetic nanofluid, ferrofluid droplet forms a stable cap shape upon contact with a solid surface, its wettability can be controlled by applying a magnetic field. In the presence of this field, the droplet can deform, split, or move, a phenomenon known as magnetowetting [143, 144].

2.7 Conclusion

In conclusion, this chapter has presented a comprehensive overview of the fundamental principles of wettability and its governing mechanisms. Key insights include:

- Fundamental concepts and definitions of wettability are introduced, providing a basis for comprehending surface-liquid interactions.
- The impact of surface roughness on wetting behavior is explained, incorporating the Wenzel and Cassie models to describe transitions between wetting regimes.
- Mathematical frameworks for droplet bouncing, electrowetting on dielectric (EWOD) systems, and the phenomenon of contact angle saturation (CAS) are highlighted.